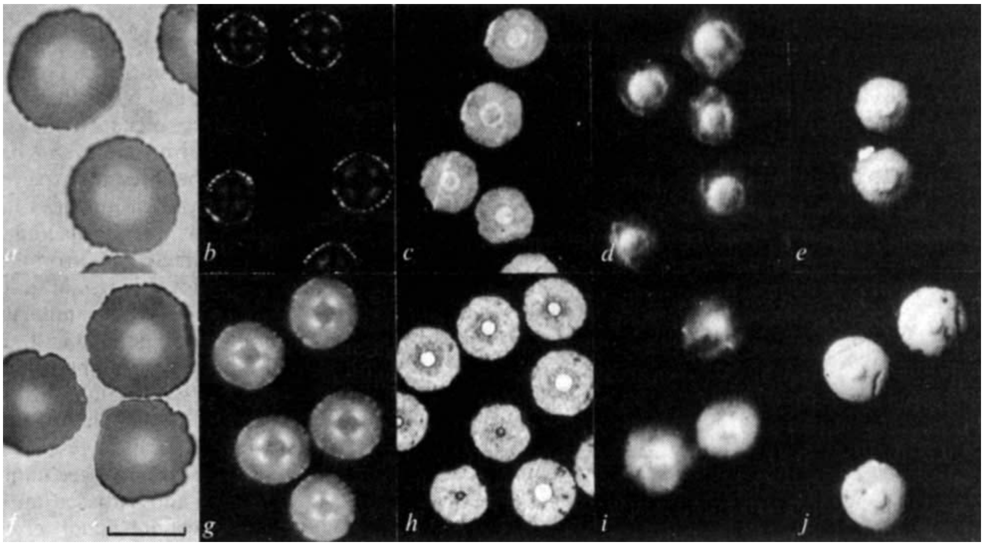

Fig. 1 Transverse fibre sections, air-oxidised at 230 °C for 30 min (*a–e*) or 2 h (*f–j*). *a,f*, Thin sections of PAN fibre before heat-treatment. *b,g*, Polarised light, 2,500 °C HTT. *c,h*, Etch colours in 2,500 °C HTT fibres. *d,i*, Etch relief in 1,400 °C HTT fibres. *e,j*, Etch relief in 1,000 C HTT fibres. Scale bar, 10 µm.

edge density in transverse sections, but these do not seem able to account for the contrast in etch rates.

In longitudinal sections intercalation will initially take place in crystallites presenting *c*-plane edges to the surface, and the depth of penetration will be limited by the crystallite width. A higher etching rate will then be associated with wider crystallites. The core is known to have greater crystallite thickness than the sheath, and it is possible that the effective crystallite width is also greater, which would account for its higher rate of etching.

Because of the high axial *c*-plane alignment all crystallites in transverse sections will be suitably oriented for intercalation. But, the rate of intercalation is expected to be greater in the less misoriented sheath where there is greater separation of lattice distortions hindering penetration. It is probable also that axial curvature and folding of layer planes produces channels in which intercalation is facilitated, and a higher density of these may accompany the smaller sheath crystallite thickness.

These ideas come some way to explaining the reversal of sheath and core etch rates in longitudinal and transverse sections. Although the etch patterns can only be correlated with what is already known of fibre fine structure, the technique is worth pursuing as a simple and sensitive monitor of morphological variations arising during the processing of PAN fibre to carbon fibre. As such it is an aid in relating strength properties to structure, and for this application a particular advantage of current controlled etching is the fact that insulating resin matrices are not attacked.

Fig. 2 Etched sections of commercial type 2 PAN-based carbon fibres. *a*, The two centre fibres show a dark core more etched than the sheath. *b*, Concentric (coloured) rings in the sheath indicate a decrease of etching outwards. Scale bar, 10 µm.

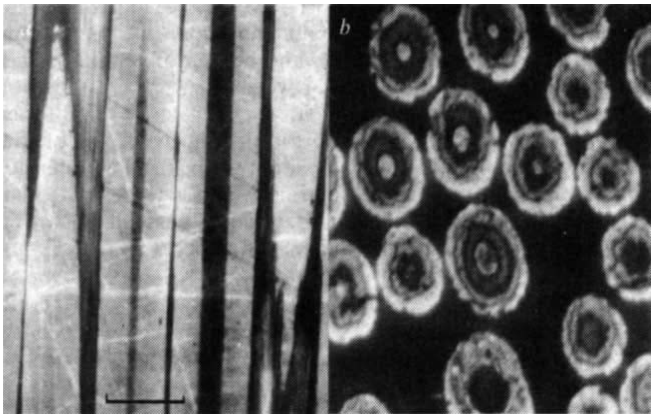

I thank W. Watt and W. Johnson of the Royal Aircraft Establishment, Farnborough for useful discussions and for providing carbon fibres and the photographs of PAN fibres.

P. W. MANDERS

Department of Metallurgy and Materials Technology,
University of Surrey,
Guildford,
Surrey, UK

Received 17 October; accepted 8 November 1977.

1. Barnet, F. R. & Norr, M. K. *Composites* **7,** 93–99 (1976).
2. Wicks, B. J. & Coyle, R. A. *J. mat. Sci.* **11,** 376–383 (1976).
3. Knibbs, R. H. *J. Microsc.* **94,** 273–281 (1971).
4. Johnson, D. J., Crawford, D. & Jones, B. F. *J. mat. Sci.* **8,** 286–290 (1973).
5. Watt, W. & Johnson, W. *Nature* **257,** 210–212 (1975).
6. Butler, B. L. & Diefendorf, R. J. Proc. 9th Biennial Conference on Carbon, Defence Ceramic Information Centre (1969), p. 161.
7. Hérinckx, C., Perret, R. & Ruland, W. ibid, p. 121.
8. Hennig, G. *J. chem. Phys.* **19,** 922–929 (1951).

Evidence for reptation in an entangled polymer melt

ENTANGLEMENTS, their nature and their role in the dynamic properties of concentrated polymer solutions and melts are not well understood[1,2]. The classical molecular view of entanglements has been one of rope-like intermolecular couplings at a number of points along the length of a molecule; molecules in motion would drag past these couplings, the essential effect being one of enhanced friction[1,3]. There has been a growing realisation that this model is inadequate[2,4,5]. The essence of the problem, rather, seems to be that of the topological restrictions imposed on the motion of each polymer molecule by its neighbours: movement of a given polymer chain is constrained at the points of entanglement or intersection with adjacent chains[2]. Theoretical treatment of the topological problem is difficult[6], and has met only with limited success[5]. An interesting proposal regarding the motion of molecules within entangled polymer systems has been put forward by De Gennes[4,7]: according to this, the motion of a given polymer molecule is confined within a virtual 'tube' defined by the locus of its intersections (or points of 'entanglement') with adjacent molecules (Fig. 1). The molecule is constrained to wriggle, snake-like, along its own length, by curvilinear propagation of length defects such as kinks or 'twists'[8] along the tube; this mode of motion has been termed reptation[4] (from reptile). Reptative motion clearly satisfies the central requirement of entangled systems: that of the non-crossability by a given chain of the contours of its adjacent

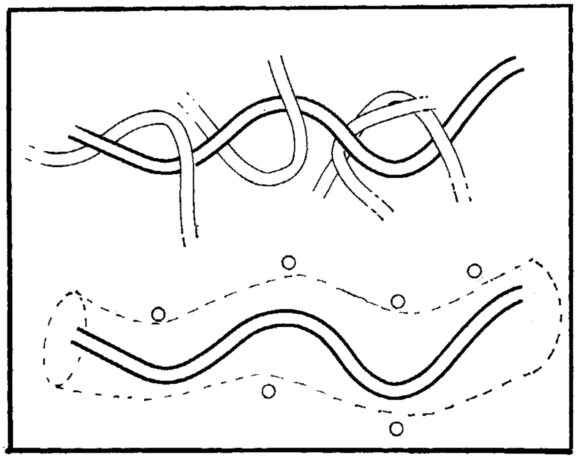

Fig. 1 A polymer chain in an entangled melt (or concentrated solution) may be regarded as being within a virtual 'tube' defined by the locus of its intersections with other melt molecules, as indicated. The obstacles defining the 'tube' in the lower figure are sections through the melt molecules in a plane parallel to the paper. For clarity, the density of segments shown is much lower than would be the case in a real melt.

neighbours. In a real polymer melt the topological environment of any given molecule (that is, the virtual 'tube' surrounding it) will itself change with time. This is because the adjacent molecules defining it are themselves mobile. If this reorganisation is sufficiently slow then the translational motion of the enclosed molecule will be effectively curvilinear (reptative). Consideration of the problem[9] suggests that this will be the case in an entangled system. One then expects translational diffusion to be dominated by reptation. There is no direct experimental evidence supporting the physical reality of curvilinear motion in entangled polymer systems. I report here the results of experiments on diffusion within a polyethylene melt critically designed to test the reptation concept.

One outcome of constraining a polymer chain of random walk configuration to diffuse, by Brownian motion, within a confining (virtual) tube, is that the translational diffusion coefficient D scales as

$$D \propto M^{-2} \qquad (1)$$

where M is the molecular weight. This may be readily proved[4], and is a direct consequence of imposing a random walk configuration on the essentially one-dimensional curvilinear diffusion of the molecule along its own contour.

Previous studies of self-diffusion in concentrated polymer solutions and in melts have involved mainly the use of NMR[10-14] and radio-tracer techniques[15-17]. The results of the NMR studies are ambiguous, as it is difficult to separate the contributions to the overall motion due to translation of the molecule as a whole from those due to the internal (segmental) motion[11,13]. McCall *et al.*[10], for example, using the NMR technique, have estimated the diffusion coefficient in molten polyethylene to vary as $D \propto M^{-5/3}$; their result, however, was based on rather limited data. In the case of the radio-tracer studies involving the variation of D with diffusant length in polymer melts, the results[15,16] have been of a somewhat qualitative nature and have lacked a discriminative character.

Table 1 Molecular weight characteristics of the deuterated polyethylene (DPE) fractions.

Fraction	M_w	M_w/M_n	(N_w)
DPE1	3,600	2.25	(225)
DPE2	4,600	2.2	(288)
DPE3	11,000	3.4	(688)
DPE4	17,000	2.2	(1,063)
DPE5	23,000	1.8	(1,438)

Characteristics were determined by gel permeation chromatography. N_w is the weight-average degree of polymerisation, corresponding to M_w.

In the present experiments the translational diffusion coefficient D of a series of deuterated linear polyethylene (DPE) fractions was measured in a protonated linear polyethylene (PPE) melt. Neutron scattering studies[18,19] of polyethylene melts, in which small amounts of DPE were dissolved in PPE (and vice versa), indicate that the radius of gyration of the minor component in the melt is consistent with its having a random coil configuration. Thus if translational diffusion of the DPE molecules within the PPE melt is taking place by reptation, the relation of equation (1) must hold: and this is what I set out to test.

The measuring technique was developed by B. J. Briscoe and myself, and is based on infrared (IR) microdensitometry; it is described in detail elsewhere[20]. In essence, the technique involves setting up a concentration step-function of the diffusant of interest within the matrix, and allowing it to broaden, with time, under diffusion. Measurement of the final diffusion broadened profile is carried out using an IR microdensitometer, which yields a value for D. The diffusant must absorb at some IR frequency unaffected by the matrix: in the present case, the labelling frequency was that of the C–D stretching mode (in DPE) at 2,170 cm^{-1}, a region free of absorption by the PPE.

Five fractions of linear DPE (98% deuterated) were used. Table 1 shows their molecular weight characteristics, as determined by gel permeation chromatography. The PPE matrix was linear polyethylene of $M_w = 1.6 \times 10^5$, $M_w/M_n \simeq 15$ and $CH_3/1{,}000C < 1$; this molecular weight is much higher than the critical molecular weight for the onset of 'entangled' behaviour, as deduced from viscosity and other measurements[1,2]. Solid solutions, 2% w/w, of each DPE fraction in the PPE matrix were prepared by dissolving and mixing both components in boiling xylene; the mixture was then precipitated from solution by pouring into cold excess methanol. After washing and drying, pellets were moulded from these precipitates and from pure PPE which had been similarly dissolved and precipitated, and these were coherently joined[20] to form composites containing a step function in DPE concentration (Fig. 2*a*). The composites were placed in suitable PTFE containers inside sealed glass ampoules under nitrogen, and left for various lengths of time at the diffusion temperature. On quenching (thereby effectively stopping further diffusion), slices were taken from the composites and scanned in the IR microdensitometer[20] to yield the diffusion broadened profiles (Fig. 2*b*).

Evaluation of D for a diffusion broadened step function is straightforward when dealing with a single diffusing species[21]. When a diffusant is not monodispersed, however, difficulties arise in interpreting the experimental data. This problem has led to serious anomalies in previous studies of self-diffusion, mainly with NMR techniques[11,12]. In the present case, the final broadened profile (such as in Fig. 2*b*) is the sum of contributions from species of different molecular weight (within each DPE fraction, see Table 1), and hence different D values. If a diffusing species of molecular weight $= M_i$ has a diffusion coefficient D_i associated with it, such that $D_i \propto M_i^{\alpha}$, then analysis shows (J.K. in preparation) that the slope of the broadened step function at the position of the original interface (Fig. 2*b*) is the experimental quantity which is to be measured. This yields an overall diffusion coefficient $\bar{D}$ associated with a diffusion-average molecular weight, M_D, such that

$$\bar{D} \propto M_D^{\alpha} \qquad (2)$$

where

$$M_D = \left(\sum_i w_i M_i^{-\alpha/2}\right)^{-2/\alpha}$$

w_i are the weight fractions of each species M_i comprising the diffusant sample.

In Fig. 3 M_w is plotted against the diffusion coefficient $\bar{D}$ as measured from the slope of the diffusion-broadened profiles such as in Fig. 2*b*. The best fit to the data is

$$\bar{D} \propto M_w^{p} \qquad (3)$$

where $p = -2.0 \pm 0.1$. But for $\alpha = -2$, M_D becomes identical with M_w: for consistency of equations (2) and (3), therefore, α must be identified with p.

Thus for a DPE molecule of molecular weight M, diffusing in an 'entangled' PPE melt, the translational diffusion coefficient D scales as

$$D \propto M^{-2 \pm 0.1}$$

This result is to be compared with the reptation relation of equation (1); it may be contrasted with the relation $D \propto M^{-3.5}$ expected on the basis of, for example, Bueche's entanglement-coupling model.

These results provide direct experimental support for the suggestion that the translational diffusion mode of polymer molecules in 'entangled' melts is a curvilinear one. This has a number of implications.

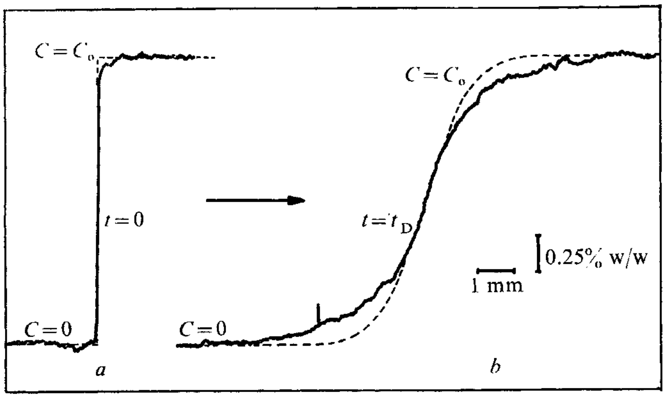

Fig. 2 Typical concentration profiles of deuterated polyethylene (DPE) in the protonated polyethylene matrix (PPE). *a*, Immediately subsequent to creation of a step-function. $C_0 = 2\%$ w/w of fraction DPE3 in PPE. The broken line represents an ideal step-function, and the continuous line is the profile as scanned in the infrared microdensitometer[18]. The scanning frequency is that of the C–D stretching mode at 2,170 cm^{-1}. *b*, The concentration profile of (*a*) following a diffusion run. Diffusion temperature $T_D = 176.0 \pm 0.3$ °C; $t_D = 1.114 \times 10^6$ s; D as evaluated from the slope at the position of the original interface, is $3.7 \pm 0.6 \times 10^{-9}$ cm^2 s^{-1}. The broken curve is the theoretical Fickian profile for a single diffusing species with the diffusion coefficient D; the deviations from the experimental profile are due to the polydispersity of the actual diffusant sample (see text and also equation (2)).

The effect of 'entanglements' on the slow relaxation modes in 'entangled' systems now seems to be clearer: the slowest of these modes corresponds to the centre-of-mass translational diffusion of the molecules, and is constrained to take place by reptation. The concept of localised entanglement coupling at a relatively small number of points, which lay at the heart of classical theory, must give way to the view where the effect of entanglements is one which pervades the length of a molecule: the net result is one of topological constraints on the motion of molecules. For sufficiently high molecular weight, curvilinear motion alone is allowed.

It is tempting to suggest, in view of these results, that the onset of snake-like motion corresponds also to the onset of entangled behaviour. This suggestion is explored elsewhere[9]. Within the range of experimental parameters described, however, the results clearly support De Gennes' notion of reptation in an entangled polymer system.

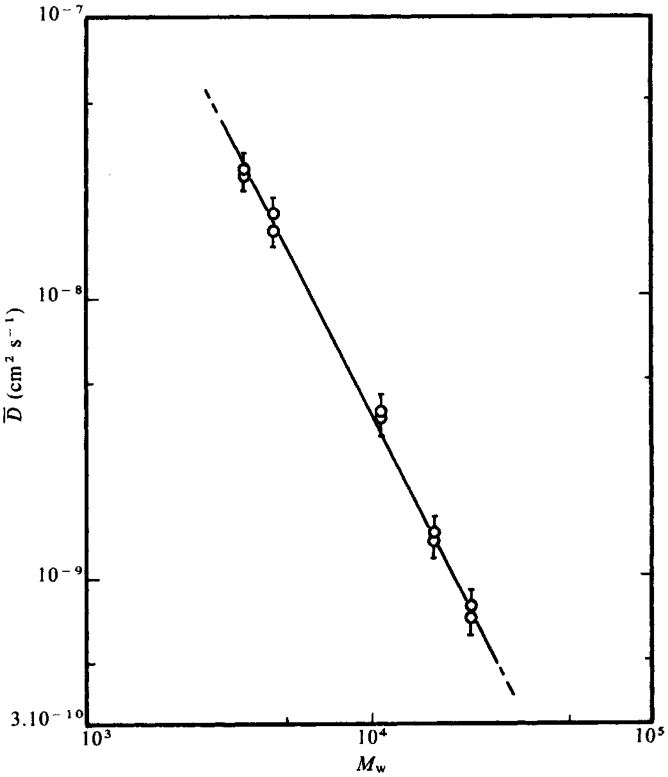

Fig. 3 The variation of $\bar{D}$ with M_w for deuterated polyethylene diffusing in a protonated polyethylene matrix, at a diffusion temperature of 176.0 ± 0.3 °C. Each point represents a separate experiment, and is the mean of 10 separate profiles such as in Fig. 2*b*. The lengths of experimental runs (t_D) vary by a factor of ~3 within each pair of experiments for a given DPE fraction. The least-squares best-fit to the data is the relation:

$$\bar{D} = 0.2\, M_w^{-2.0 \pm 0.1}, \text{ and is shown.}$$

I thank Professor Sir S. F. Edwards for stimulating discussions, Dr D. G. Ballard and Dr G. Longman for supplying the deuterated fractions, and Professor D. Tabor and Dr B. J. Briscoe for their encouragement. A grant from Dow Corning Chemicals and a Research Fellowship from St Catharine's College, Cambridge, are both gratefully acknowledged.

J. KLEIN*

Physics and Chemistry of Solids,
Cavendish Laboratory,
Madingley Road, Cambridge, UK

Received 7 July; accepted 4 November 1977.

*Present address: Polymer Department, Weizmann Institute of Science, Rehovot, Israel.

1. Ferry, J. D. *Viscoelastic Properties of Polymers* 2nd edn (Wiley, London, 1970).
2. Graessley, W. W. *Adv. pol. Sci.* **16**, 1–179 (1974).
3. Bueche, F. *J. chem. Phys.* **20**, 1959–1964 (1952); *Physical Properties of Polymers* (Interscience, London, 1962).
4. De Gennes, P. G. *J. chem. Phys.* **55**, 572–579 (1971).
5. Edwards, S. F. & Grant, J. W. V. *J. Phys.* **A6**, 1169–1185 (1973).
6. Edwards, S. F. *Proc. phys. Soc.* **91**, 513–519 (1967).
7. De Gennes, P. G. *Macromolecules* **9**, 587–598 (1976).
8. Reneker, D. H. & Fanconi, B. *J. appl. Phys.* **46**, 4144–4147 (1975).
9. Klein, J. *Macromolecules* (submitted).
10. McCall, D. W., Douglass, D. C. & Anderson, E. W. *J. chem. Phys.* **30**, 771–773 (1959); *J. pol. Sci.* **A1**, 1709–1720 (1963).
11. McCall, D. W. & Huggins, C. M. *Appl. Phys. Lett.* **7**, 153–154 (1965).
12. Tanner, J. E., Lui, K.-J. & Anderson, J. E. *Macromolecules* **4**, 586–588 (1971).
13. Tanner, J. E. *Macromolecules* **4**, 748 (1971).
14. Cosgrove, T. & Warren, R. F. *Polymer* **18**, 255–258 (1977).
15. Bueche, F., Cashin, W. & Debye, P. *J. chem. Phys*, **20**, 1956–1959 (1952).
16. Skewis, J. D. *Rubb. Chem. Technol.* **39**, 217–225 (1966).
17. Bueche, F. *J. chem. Phys.* **48**, 1410–1411 (1968).
18. Lieser, G., Fischer, E. W. & Ibel, K. *J. Pol. Sci. Pol. Lett.* **13**, 39–43 (1975).
19. Schelten, J., Ballard, D. G. H., Wignall, G. D., Longman, G. & Schmatz, W. *Polymer* **17**, 751–757 (1976).
20. Klein, J. & Briscoe, B. J. *Nature* **257**, 386–7 (1975); *Polymer* **17**, 481–484 (1976).
21. Crank, J. *Mathematics of Diffusion* 2nd edn (Oxford University Press, London, 1975).